A Molecularly Imprinted Polymer-Based Electrochemical Sensor for Heart Failure Detection

P. Longsompurana and R. P. Pooarporn*

***Abstract*—The number of Heart Failure (HF) patients is increasing every year, which suggests that early BNP detection is necessary. It is highly desired to look for a new sensor because the Brain Natriuretic Peptide (BNP) has the potential to be a cardiac biomarker for the diagnosis of HF. Due to this, the goal of this study was to create and develop a novel electrochemical sensor for BNP detection based on Molecularly Imprinted Polymer (MIP) rather than an antibody. The modification of carbon Screen Printed Electrode (SPCE) using functionalized-multiwall carbon nanotube/tris (bipyridine) ruthenium (II) chloride (f-MWCNTs/Ru) composites has the advantage of improving the electrode's electron transfer process, as effectively shown by the Cyclic Voltammogram (CV). Pyrrole (Py) and pyrrole-3-carboxylic acid (Py3C) were used as a copolymeric matrix to create the BNP recognition sites. BNP and two monomers were electropolymerized together in a single step by CV method. Differential Pulse Voltammetry (DPV) was used to determine the optimum conditions for the MIP-based BNP sensor, including the Py: Py3C ratio, the number of electropolymerizations, the rebinding pH, and the rebinding time. The DPV results of the new MB labeled NPs revealed directly proportional to the concentrations of rebinding BNP from 10 to 500 pg.cm^{-3} under optimal conditions, making them acceptable for the detection of both chronic and acute HF. This approach provides an improved detection range and may provide a novel and efficient platform for protein biomarkers.**

***Index Terms*—Brain Natriuretic Peptide (BNP), electrochemical sensor, Molecularly Imprinted Polymer (MIP)**

I. Introduction

Heart Failure (HF) occurring in cardiovascular disease is a major cause of death, and the number of people living with the heart failure is rising [1]. Patients with HF usually have nonspecific symptoms. According to conventional procedures, a patient's evaluation is based on various methods such as their medical history, physical examination, and chest X-ray. However, blood test has been used in laboratory for conducting evolutionary study. Accordingly, the main biomarkers for HF detection such as Creatinine Kinase (CK), troponin T (TnT), Brain Natriuretic Peptide (BNP), etc. Especially, BNP is an internationally recognized biomarker in the diagnosis of HF and clinical practice [2] based on cut-off point level of 35 pg.cm^{-3} and 100 pg.cm^{-3} for chronic and acute HF, respectively [3]. There are several traditional techniques for BNP detection based on immune/antigen reaction assay such as immunoradiometric assays, micro-mosaic immunoassays, Resonance Energy Transfer (ECL-RET) immunosensor, and surface plasmon resonance (SPR)-based immunosensor. However, these techniques are considered time-consuming processes due to their complexities in operation, and expensive equipment [4]. Moreover, these techniques must apply the antibody which its conformation is limited by inefficiency and inaccuracy of the detection [5]. Therefore, Molecularly Imprinted Polymer (MIP) has been studied as an option for mimicking antibody which provides an effective strategy for detection by using inexpensive reagents, providing stability, quick response, and reproducible materials [5]. Subsequently, MIP is an important component in biosensor development, and plays a key role in analytical target binding. Thus, the MIP-based electrochemical sensor is an effective alternative sensor for cardiac biomarker sensing. Recently investigators have examined the effects of non-conductive polymer i.e., acrylamide as monomer and N, N-methylenebisacrylamide as cross-linker were synthesized the MIP on f-MWCNTs for TnT sensing providing the linear range of detection which was not satisfied for cut-off level [6]. Accordingly, there is concerning that some non-conductive polymers are being disadvantaged and until recently, there has been no study for MIP-based electrochemical sensors. Thus, this study mainly focused on conductive polymer which are Py and Py3C [7] for generating MIP-based BNP sensor.

Basically, the BNP peptide is a non-electrochemical analyte which cannot directly provide the electrochemical signal. For this reason, a new electrochemical enhancer nanoparticle (NPs) which was MB/βCD/BNPapt/Ag@SiO_2 NPs (we called the MB labeled NPs) was proposed to enhance the electrochemical signal for the MIP-based BNP sensor. Since the Methylene Blue (MB) is an organic redox probe that can be encapsulated in heptakis (6-deoxy-6-thio)-beta-cyclodextrin (βCD) host molecules and actively provide an electrochemical signal [8] corresponding to BNP.

In addition, to conduct the specific binding between MB labeled NPs and BNP peptide, the BNP aptamer (BNPapt) was deliberately chosen as a specific BNP capture molecule [9] and attached to MB labeled NPs as well. With this intention, the MB labeled NPs were obtained to perform sandwich assays for MIP-based BNP sensor, efficiently.

II. Materials and Methods

A. f-MWCNTs/Ru-Modified SPCE Fabrication

The f-MWCNTs and Ru were mixed in 40% ethanol under ultrasonication. Then the f-MWCNTs/Ru nanocomposite was washed and dried at room temperature. It was well prepared for 0.1 mg.cm^{-3} in 40% ethanol. Next, the nanocomposite suspension was dropped on the working electrode of SPCE to obtain the f-MWCNTs/Ru/SPCE for MIP-based BNP sensor fabrication.

Manuscript received December 5, 2022; revised March 10, 2023, accepted May 11, 2023.

P. Longsompurana and R. P. Pooarporn are with the Biological Engineering Program, Faculty of Engineering, King Mongkut's University of Technology Thonburi, Thailand. E-mail: phoomintara.long@mail.kmutt.ac.th (P.L.)

*Correspondence: rungtiva.pal@kmutt.ac.th (R.P.P.)

B. Fabrication of a MIP-Based BNP Sensors

To fabricate the MIP-based BNP sensors, the solution of Py and Py3C monomers (0.01 mol.L^{-1}), and BNP template (10 µg.cm^{-3}) in phosphate buffer solution (PBS) (0.01 mol.L^{-1}, pH 6.8) was deposited on the modified electrode. To provide the interactions between the BNP template and monomers, the mixture was incubated at 4 ºC for one hour. After being incubated, its solution was electropolymerized on the surface by CV technique in the potential range from 0.4 to 1.0 V and a scan rate of 0.02 V.s^{-1}. Finally, the sensor was immersed in oxalic acid (Oxa) solution overnight to remove the BNP template. The resulting MIP-based BNP sensor was obtained for further electrochemical experiments. For the control study, the Non-Imprinted Polymer (NIP) was prepared by the same approach of MIP fabrication without BNP template.

C. MB Labeled NPs Production

SiO_2 NPs were synthesized using the Stöber method from the sol-gel process of ethanol, DI water, 25% NH_4OH, and tetraethyl orthosilicate (TEOS) under continuously stirring for one hour. The resulting SiO_2 NPs were collected by centrifugation and redispersed in DI water. A 0.7 cm^3 of freshly prepared $[Ag(NH_3)_2]^+$ solution (500 µL of 0.02 mol.L^{-1} $AgNO_3$, 100 µL of 0.1 mol.L^{-1} NaOH, and 100 µL 25% NH_4OH) was quickly added to the SiO_2 NPs suspension. The glucose solution of 0.1 mol.L^{-1} was then immediately added suspension and continuously shaken for three hours. The $Ag@SiO_2$ NPs were collected by centrifugation.

The resulting $Ag@SiO_2$ NPs were further resuspended in PBS pH 7.0. Ten µL of 100 nmol.L^{-1} BNPapt, 0.1 mmol.L^{-1} βCD, and 10 µmol.L^{-1} tris(2-carboxyethyl) phosphine (TCEP) were added to the $Ag@SiO_2$ NPs suspension and continuously shaken overnight. βCD/BNPapt/$Ag@SiO_2$ NPs were acquired and then resuspended in 1 cm^3 PBS pH 7. Ten µL of 1 mmol.L^{-1} MB solution was added to the NPs suspension and shaken overnight to allow the MB absorption into the βCD. Finally, the MB/βCD/BNPapt/$Ag@SiO_2$ (MB labeled NPs) were then washed in DI water several time to remove unbound MB and resuspended again in PBS.

D. Electrochemical Measurements

Electrochemical measurements were operated by Autolab PGSTAT128N (Metrohm) with NOVA 2.1 software. The f-MWCNTs/Ru/SPCE, MIP/f-MWCNTs/Ru/SPCE, and NIP/f-MWCNTs/SPCE were investigated by CV technique with the scan rate of 0.05 V.s^{-1}. The DPV technique was used for the optimization of Py:Py3C ratio (5:1, 2.5:1, 1:1, 1:2.5, and 1:5), number of electropolymerization cycle (10, 15, 20, 25, and 30 cycles), rebinding pH (5, 6, 7, 8, and 9), and binding time (15, 30, 45, 60, and 75 minutes). All experiments were operated in 100 µL $K_3[Fe(CN)_6]$/$K_4[Fe(CN)_6]$ 2.5 mmol.L^{-1} (1:1) containing 0.1 mol.L^{-1} KCl. The ΔI represents the rebinding performance which was calculated by Eq. (1).

$$\Delta I = I_{\text{after rebinding}} - I_{\text{before rebinding}} \quad (1)$$

The calibration curve was operated by sandwich assay under optimal conditions. The BNP at 10, 100, 250, and 500 pg.cm^{-3} were incubated with MB labeled NPs on MIP-based BNP sensor at room temperature for one hour. The unbound was washed with PBS. The electrochemical responses were measured by DPV in PBS pH 7.

E. Structural and Morphological Characterization

The Atomic Force Microscopy (AFM) was performed in noncontact mode at an area of 500 nm × 500 nm to investigate micrographs. Next, the roughness was analyzed by XEI 4.3.4 build 22 software.

III. Results and Discussion

A. Characterization of the Modified SPCE

The electrochemical properties of nanocomposite were studied using the CV technique. Fig. 1(a) showed the comparison of CV profiles for three different electrodes which were SPCE (I), f-MWCNTs/SPCE (II), and f-MWCNTs/Ru/SPCE (III), obtained at 2.5 mmol.L^{-1} $K_3[Fe(CN)_6]$/$K_4[Fe(CN)_6]$ containing 0.1 mol.L^{-1} KCl. All three electrodes exhibited well-defined redox peak with an anodic peak potential (E_{pa}) at 0.33 V, 0.31 V, and 0.25 V and cathodic peaks potential (E_{pc}) at 0.06 V, −0.03 V, and 0.01 V for bare SPCE (I), f-MWCNTs/SPCE (II), and f-MWCNTs/Ru/SPCE (III), respectively. Comparing with the bare SPCE (I), the effect of the f-MWCNTs (II) and f-MWCNTs/SPCE (III) showed higher current peak. As shown in Fig. 1(b), the f-MWCNTs/Ru/SPCE displayed higher average CV current signals than bare SPCE and f-MWCNTs/SPCE, significantly. Because of Ru^{2+} ion as a transition metal element and f-MWCNTs as conductive carbon-based material made up the nanocomposite, which can improve the electron transfer process and higher conductive specific area. Moreover, the nanocomposite demonstrates a reversible capacity after 30 cycles, the peak current decreased only 3.1% of the initial response indicating that significantly exhibits good competent cycling stability and reversibility (inset in Fig. 1(a)) without leakage of nanocomposite from the electrode surface. Accordingly, after modifying the electrode with f-MWCNTs/SPCE, a pair of well-defined reversible redox peaks was clearly observed which indicated that nanocomposite was strongly immobilized on SPCE via van der Waals interaction between f-MWCNTs/Ru and the surface of the working electrode [10, 11] resulting in increasing the stability of the sensor.

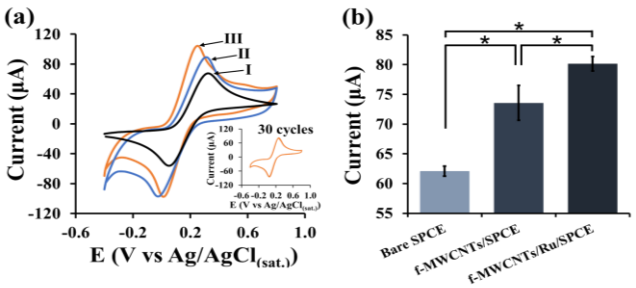

Fig. 1. Cyclic voltammogram (a) of bare SPCE (I), f-MWCNTs/SPCE (II), f-MWCNTs/Ru/SPCE (III), and f-MWCNTs/Ru/SPCE on continuously scanning 30 cycles (inset). The average of CV current signals (b) in 2.5 mmol.L^{-1} $K_3[Fe(CN)_6]$/$K_4[Fe(CN)_6]$ (1:1) containing 0.1 mol.L^{-1} KCl (scan rate 50 mV.s^{-1}) (* p-value < 0.05, One-way ANOVA, N=3, Mean ± SD).

B. Characterization of the MIP-Based BNP Sensor

The monomers are very important compounds to earn more selective and sensible MIP. Firstly, the conductive property of the monomers allowed the electron transfer process. Secondly, the functionalized organic monomers were appropriately used to form MIP-specific pocket sites to provide the strong interaction between the BNP and MIP. According to a previous study, the Py and Py3C monomers effectively exhibited the performance of the Troponin T (TnT) sensing [7]. Therefore, in this present study, the Py and Py3C were selected for MIP-based BNP sensor development. Because Py and Py3C are five-member aromatic rings that contain the amino group, and Py3C contains functionalized carboxylic group as well [7].

Fig. 2 represented the stepwise of the NIP- and MIP-modified electrodes which were performed in 2.5 mmol.L^{-1} $K_3[Fe(CN)_6]/K_4[Fe(CN)_6]$ containing 0.1 mol.L^{-1} KCl by adopting CV technique. Both MIP and NIP after polymerization (I), they were observed a decrease in redox peaks in the CV due to the polymer being deposited on nanocomposite resulting in hindering the electron transfer process. Subsequently, in the template removal step (II), MIP increased redox peaks larger than NIP due to the BNP template in MIP pocket sites being removed from the polymer to show the precise functional MIP recognition sites and enable the charge transfer process as opposed to NIP. As well as the step of the BNP rebinding process (III), the MIP displayed a current signal that was noticeably higher than NIP. As has been proved that the BNP was accessible into the MIP via hydrogen bonding and electrostatic interaction between the amino and carboxylic groups inside the MIP pocket and the amino acid side chains of the BNP [7].

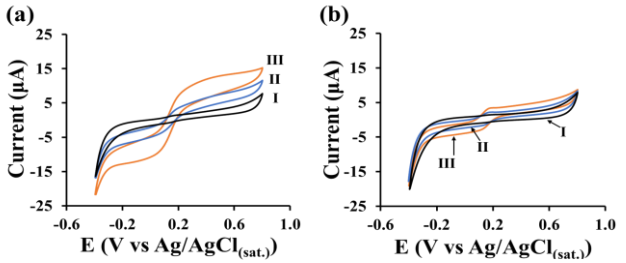

Fig. 2. CV profile of constructing stepwise of MIP (a) and NIP (b) in 2.5 mmol.L^{-1} $K_3[Fe(CN)_6]/K_4[Fe(CN)_6]$ (1:1) containing 0.1 mol.L^{-1} KCl (scan rate 50 mV.s^{-1}); after polymerization of Py:Py3C (1:1) (I), after removal of the BNP by 5 mmol.L^{-1} Oxa (II), and after rebinding with 500 pg.cm^{-3} BNP (III).

To investigate the success of MIP pocket production, the surface roughness of MIP and NIP was proved by the AFM technique as shown in Fig. 3(a) and Fig. 3(b) for MIP/f-MWCNTs/Ru/SPCE and NIP/f-MWCNTs/Ru/SPCE, respectively. The AFM image showed the tubular nanofiber shape and diversified direction for both MIP and NIP. Additionally, the Further analysis for surface roughness of MIP/f-MW CNTs/Ru/SPCE and NIP/f-MWCNTs/Ru/SPCE was 2.1±0.57 nm and 1.3±0.44 nm, respectively as shown in Fig. 3(c) indicated an increased overall roughness in the case of MIP, with a difference in height for the imprinted surface than NIP, significantly. Because the BNP template was taken out of the MIP polymer to provide the MIP pocket sites. The result confirmed that the MIP pockets were successfully created on the f-MWCNTs/Ru nanocomposite [12, 13].

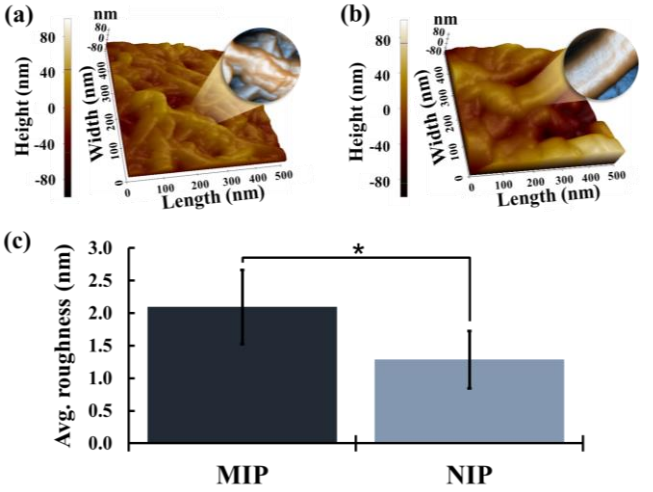

Fig. 3. AFM image of MIP/f-MWCNTs/Ru/SPCE (a) and NIP/f-MWCNTs/Ru/SPCE (b). The average surface roughness (c) after removal of the BNP by 5 mmol.L^{-1} Oxa (* p-value < 0.05, independent t-test, N=30, Mean ± SD).

C. Performance of MIP-Based BNP Sensor

The interaction between BNP and MIP recognition site is directly dependent on several factors which are functional groups, the thickness of MIP film, rebinding pH, and rebinding time. Thus, these contributing factors might be optimized for the highest efficiency. Hence, optimal experimental parameters were established through the ΔI value as in Eq. (1) after rebinding with BNP (500 pg.cm^{-3}).

All things considered, the polymerizable monomer was the first factor that directly bonded to the BNP template molecule by noncovalent interaction, it would be the most important factor affecting the recognition properties of MIP. To evaluate the specific MIP pocket sites, the functional groups which were the amino and the carboxylic group were carefully designed by varying the ratio of Py and Py3C in the step of pre-assembling incubation with BNP template for MIP-based BNP sensor fabrication. The binding performance of each ratio was carried out through the difference of current value (ΔI). After the rebinding process, the DPV results showed a maximum value when the Py and Py3C were found at 1:1 which was the highest ΔI, significantly as shown in Fig. 4(a).

The second important factor is the film thickness of the MIP recognition sites that affects the recognition ability in MIP-based BNP sensor. It can be performed by electropolymerization cycles using CV technique after pre-assembling step. Fig. 4(b) expressed the copolymeric matrix grew up correlating with the cycle of electropolymerization from 10 to 20 cycles. On the contrary, after 20 cycles, the signal decreased and led to form the thicker film with less accessible imprinted sites. As a result, at 20 cycles of electropolymerization demonstrated a maximal current response, significantly. It was selected as the ideal number of cycles to properly generate MIP thickness for BNP rebinding.

Another important to realize, rebinding pH solution

provided a direct impact on the BNP and MIP conformation. Accordingly, the MIP was fabricated under the optimal conditions of Py:Py3C (1:1) and electropolymerization (20 cycles). After BNP rebinding step, the binding affinity was investigated by DPV. As shown in Fig. 4(c), pH 7.0 was proved to be the most favorable for interaction between BNP and MIP. Because the BNP peptide and MIP are in their optimum configuration under these conditions, which have a biologically neutral pH. At this pH, the amino group of some amino acids of BNP e.g., lysine and arginine were protonated to form the positive charge. In the other hand, the carboxylic group of Py3C and some amino acids of BNP e.g., aspartate and glutamate were deprotonated to form negative charge. Under these circumstances, MIP and BNP provided the optimal binding via electrostatic and hydrogen bond interaction.

In the final performance analysis, Fig. 4(d) showed the incubation times of BNP on MIP. MIP-based BNP sensors were prepared under the optimal conditions of Py:Py3C (1:1), electropolymerization (20 cycles), and rebinding pH of 7.0 as well. The BNP was incubated in various incubation time from 15 to 75 minutes, the ΔI was calculated from the DPV peak currents after rebinding step. The results exhibited an optimal time of 60 minutes. According to all optimum investigated parameters, these conditions were approximately used for BNP sandwich assay in further study.

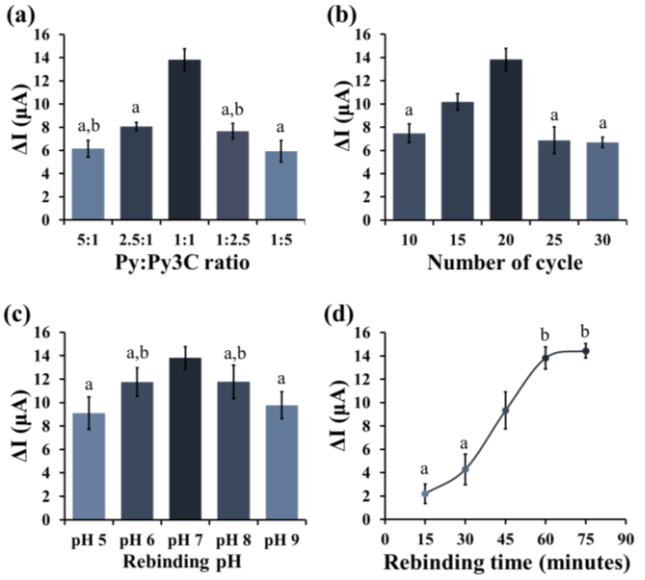

Fig. 4. Influence of Py:Py3C ratio (a), number of electropolymerization cycle (b), rebinding pH (c), and rebinding time (d). The ΔI values obtained of DPV analysis in 2.5 mmol.L^{-1} $K_3[Fe(CN)_6]/K_4[Fe(CN)_6]$ (1:1) containing 0.1 mol.L^{-1} KCl after rebinding with 500 pg.cm^{-3} BNP; all experiments performed by DPV technique (α 0.05, One-way ANOVA, N=3, Mean ± SD).

D. Electrochemical Property of MB Labeled NPs

DPV was utilized to determine the electrochemical behavior of MB labeled NPs. We can observe the oxidation current signal change of diverse nanoparticles. Fig. 5(a) exhibits the comparing the DPV of PBS pH 7 (I), SiO_2 NPs (II), $Ag@SiO_2$ NPs (III), βCD/BNPapt/$Ag@SiO_2$ NPs (IV), and MB labeled NPs (V) on bare SPCE. As expected, only the electrode with MB labeled NPs showed the characteristic oxidation peak at −0.38 V [8], whereas the PBS and other NPs without MB (I to IV) did not express the DPV peak current. In the hope that the optimum pH of the solution must provide the maximum peak, the pH value of MB labeled NPs reaction was evaluated by measuring the DPV responses of MB labeled NPs on bare SPCE. As given in Fig. 5(b), it presented that the oxidation peak current changed increasingly (from pH 5.0 to 7.0) and then decreased for higher pH values. Then, pH 7.0 was chosen for adopting as the MB labeled NPs in all subsequent analytical BNP sandwich assay in the next step.

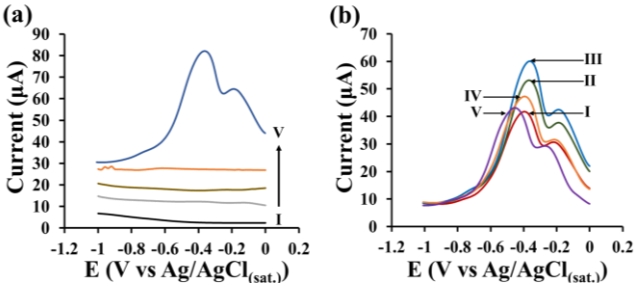

Fig. 5. DPV spectra (a) of PBS (I), SiO_2 NPs (II), $Ag@SiO_2$ NPs (III), βCD/BNPapt/$Ag@SiO_2$ NPs (IV), and MB labeled NPs (V) in PBS pH 7.0. The effect of pH for reaction of MB labeled NPs (b) from pH 5 (I) to 9 (V).

E. Determination of Linear Range by Sandwich Assay

The analytical performance of the sensor was evaluated by submitting the BNP diluted in PBS pH 7.0 with the same concentration of MB labeled NPs on the MIP-based BNP sensor to conduct the sandwich assays. As shown in Fig. 6(a), the electrochemical responses of MB labeled NPs were obtained by using the DPV measurement in PBS pH 7.0. As expected, the oxidation peak current responses of MB labeled NPs proportionally correlated with the concentration of BNP. Consequently, the resulting calibration plot in Fig. 6(b) was linear over the range from 10 to 500 pg.cm^{-3}. The corresponding linear regression equations was I (μA) = 0.74log[BNP] + 1.08 (R^2 = 0.9668).

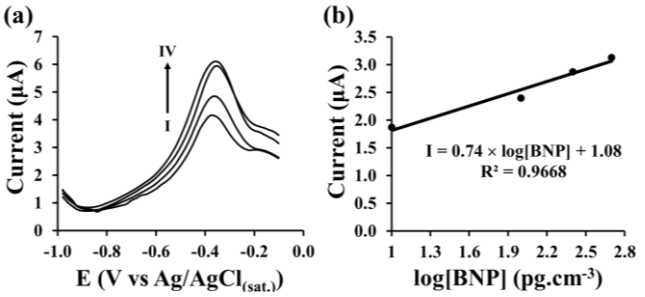

Fig. 6. The DPV response in PBS pH 7.0 of MB labeled NPs for BNP detection after BNP rebinding from 10 pg.cm^{-3} (I) to 500 pg.cm^{-3} (IV) (a). The calibration curve of BNP sensing (b).

IV. Conclusions

As expected, the f-MWNTs/Ru nanocomposite was successfully modified on SPCE, this nanocomposite was carefully examined in order to provide a high surface area and improve accelerated conductivity and sensitivity. Furthermore, the functionalized conductive polymers substantially improved the performance of the MIP-based BNP sensor. Finally, the novel MB labeled NPs may have

improved the electrochemical signal for trustworthy sensing. Accordingly, the MIP-based BNP sensor was successfully designed to improve potential HF detection.

Conflict of Interest

The authors declare no conflict of interest.

Author Contributions

Conceptualization, R.P.P.; methodology, R.P.P. and P.L.; validation, P.L.; investigation, P.L.; writing—original draft preparation, P.L.; writing—review and editing, R.P.P.; visualization, P.L. All authors have read and agreed to the published version of the manuscript.

Funding

This research project is funded by National Research Council of Thailand (NRCT) and King Mongkut's University of Technology Thonburi: N42A650316 and supported by Thailand Science Research and Innovation (TSRI). Basic Research Fund: Fiscal year 2022 under project number FRB650048/0164.

Acknowledgment

P. Longsompurana would like to thanks to Petchra Pra Jom Klao Ph.D. Research Scholarship from King Mongkut's University of Technology Thonburi.

References

[1] A. Groenewegen, F. H. Rutten, A. Mosterd, and A. W. Hoes, "Epidemiology of heart failure," *Eur. J. Heart Fail.*, vol. 22, no. 12, pp. 1342−1356, Aug. 2020.

[2] H. K. Gaggin and J. L. Januzzi Jr, "Biomarkers and diagnostics in heart failure," *Biochim. Biophys. Acta*, vol. 1832, no. 2, pp. 2442–2450, Dec. 2013.

[3] P. Ponikowski *et al.*, "2016 ESC guidelines for the diagnosis and treatment of acute and chronic heart failure," *Eur. Heart J.*, vol. 37, no. 27, pp. 2129–2200, July 2016.

[4] T. Dahiya, S. Yadav, N. Yadav, A. Mann, M. Sharma, and J.S. Rana, "Monitoring of BNP cardiac biomarker with major emphasis on biosensing methods: A review," *Sensors International*, vol. 2, 100103, June 2021.

[5] G. Zhang *et al.*, "Precise detection of prostate specific antigen in serum: A surface molecular imprinted sensor based on novel cooperated signal amplification strategy," *Sensors and Actuators B: Chemical*, vol. 302, 1269981, Jan. 2020.

[6] F. T. C. Moreira, R. A. F. Dutra, J. P. C. Noronha, A. L. Cunha, and M. G. F. Sales, "Artificial antibodies for troponin T by its imprinting on the surface of multiwalled carbon nanotubes: its use as sensory surfaces," *Biosens. Bioelectron.*, vol. 28, no. 1, pp. 243–250, Oct. 2011.

[7] B. V. M. Silva, B. A. G. Rodríguez, G. F. Sales, M. D. P. T. Sotomayor, and R. F. Dutra, "An ultrasensitive human cardiac troponin T graphene screen-printed electrode based on electropolymerized-molecularly imprinted conducting polymer," *Biosens. Bioelectron.*, vol. 77, pp. 978–985, Mar. 2016.

[8] R. Zhang, Y. Zhang, X. Deng, S. Sun, and Y. Li, "A novel dual-signal electrochemical sensor for bisphenol A determination by coupling nanoporous gold leaf and self-assembled cyclodextrin," *Electrochimica Acta*, vol. 271, pp. 417–4241, May 2018.

[9] I. Grabowska *et al.*, "Electrochemical aptamer-based biosensors for the detection of cardiac biomarkers," *ACS Omega*, vol. 3, no. 9, pp. 12010−12018, Sep. 2018.

[10] S. T. R. Naqvi *et al*., "Modification strategies for improving the solubility/dispersion of carbon nanotubes," *J. Mol. Liq.*, vol. 297, 111919, Jan. 2020.

[11] S.-H. Oh *et al*., "Nanophotonic biosensors harnessing van der Waals materials," *Nat. Commun.*, vol. 12, p. 3824, Dec. 2021.

[12] J. P. Rosengren-Holmberg *et al.*, "Heparin molecularly imprinted surfaces for the attenuation of complement activation in blood," *Biomater. Sci.* vol. 3, pp. 1208–1217, Aug. 2015.

[13] C. E. Buensuceso *et al.*, "Electropolymerized-molecularly imprinted polymers (E-MIPS) as sensing elements for the detection of dengue infection," *Anal. Bioanal. Chem.*, vol. 414, no. 3, pp. 1457–1458, Jan. 2022.